PHYSICAL REVIEW A VOLUME 41, NUMBER 10 15 MAY 1990

Relative rotation rates: Fingerprints for strange attractors

N. B. Tufillaro
Department of Physics, Bryn Mawr College, Bryn Mawr, Pennsylvania 19010-2899

Hernán G. Solari and R. Gilmore
Department of Physics and Atmospheric Science, Drexel University, Philadelphia, Pennsylvania 19104-9984

(Received 16 March 1990)

Chaotic dynamics on a strange attractor of low dimensionality can be characterized by a set of recently proposed topological invariants. These are the relative rotation rates of the unstable periodic orbits embedded in the strange attractor. We demonstrate the efficiency of this characterization by extracting the topological invariants from chaotic time-series data for the Duffing oscillator.

At the onset of low-dimensional chaotic behavior, strange attractors are characterized by metric as well as topological universality.[1-4] Although metric universality holds only at the onset of chaos, there is growing evidence that some aspects of strange invariant sets can be characterized by universal topological properties.[5-7] These topological invariants are derived from the unstable periodic orbits embedded in strange attractors. Unstable periodic orbits are densely embedded in, and provide a good characterization of, hyperbolic strange invariant sets.[8] Even in nonhyperbolic strange sets, it seems that a knowledge of the periodic orbits and their organization should severely constrain the dynamics and recurrence properties of the strange set. We show in this Rapid Communication that a relatively small number of periodic orbits is sufficient not only to characterize a strange attractor but to determine its global torsion as well.

Three approaches to characterizing the invariant topological properties of strange attractors are based on the unstable periodic orbits within the strange set. Each requires the reconstruction of periodic orbits from a time series generated by the chaotic dynamics of a strange attractor. They differ by successively extracting more topological structure from the strange set.

In one approach[9-11] the spectrum of periodic orbits reconstructed from maps is determined. From this information and the eigenvalues of these orbits, the invariant measure, fractal dimension, and Lyapunov exponent can be estimated.[8,10,12,13] Although this is important dynamical information it does not lead to a topological classification of the strange attractor. This can be seen in the development of the Smale horseshoe as is found, for example, in the Henon map.[14] The stretching and folding in the Henon map becomes more severe as the parameters of the map are increased. The number of orbits of a given period also changes as the return map approaches hyperbolicity. Further, the study of maps is not equivalent to the study of flows, which more properly model real experimental data. The additional piece of information required to lift a map to a flow is the global torsion.[15]

A more refined approach extends the first by attempting to determine how the periodic orbits of flows are organized among themselves. This is done by computing the knot types and linking numbers for all periodic orbit pairs.[16,17] This approach provides some information about topological organization, but is too coarse for a complete characterization as it gives up phase information between orbit pairs, and as a result also loses dynamical information.

A yet more refined approach involves computing the relative rotation rates[18,19] between all pairs of reconstructed periodic orbits. Given two periodic orbits X_A and X_B of periods p_A and p_B, which intersect a Poincaré section at $\{X_A^i\}$ and $\{X_B^j\}$ (where i and j are ordered as successive iterations of the map), the relative rotation rate $R_{ij}(A,B)$ between these orbits is defined as the average number of rotations of one orbit around the other, per period, starting from the initial conditions $\{X_A^i\}$ and $\{X_B^j\}$. This topological index preserves dynamical information by preserving phase information. The sum, over all initial conditions (ij), of $R_{ij}(A,B)$ between two orbits is their linking number, $\sum R_{ij}(A,B) = L(A,B)$. This integer is the number of times one periodic orbits winds around the other. The dynamical index $R_{ij}(A,B)$ provides additional phase information not contained in the more familiar topological index $L(A,B)$.[18] In addition, the index $R_{ij}(A,B)$ is robust during the evolution of the strange set. Once the orbits X_A and X_B exist, their relative rotation rates are fixed as long as both orbits continue to exist, independent of changes in their stability and bifurcations which create or annihilate other orbits. That is, the relative rotation rates are independent of whether the strange set is hyperbolic. An intertwining matrix, or table of relative rotation rates, of the low period orbits can be used to identify, or "fingerprint," the first return map of the strange attractor. The relative rotation rates for a flow can be computed from the return map of the flow. They are unique up to an overall additive integer, the global torsion, which describes how often the return map pivots around its axis as the flow propagates between successive Poincaré sections. The linking numbers and relative rotation rates for all pairs of periodic orbits embedded in a strange attractor are sufficient to identify uniquely the return mapping mechanism (i.e., Smale horseshoe, annulus map, iterated horseshoe) responsible for the creation of the strange attractor.

Periodic orbits for a flow are reconstructed from discretely sampled time-series data $\mathbf{x}(i)$ using a straightforward procedure.[20] The time-series data are scanned for close returns (strong recurrence properties),

$$d[\mathbf{x}(i)-\mathbf{x}(i+n)]<\epsilon . \quad (1)$$

Typically, the number of sample steps n between close returns is an integer multiple of some smallest n_0, which can be associated with the fundamental period of a periodically driven dynamical system. Segments of period $k(=n/n_0)$ are compared, and those which remain close throughout an entire period are associated with the same unstable periodic orbit of period k. This unstable orbit is estimated, or reconstructed, by choosing the orbit with the best recurrence properties (minimum ϵ), by averaging all nearby segments or by using more sophisticated least-squares return map estimates on padded segments. Once a set of reconstructed orbits of low periodicity has been extracted from the chaotic time series data, the relative rotation rates of all orbit pairs are computed. Comparison of this matrix of topological indices with intertwining matrices based on standard return maps (Smale horseshoe, iterated horseshoe, annulus map[21]) is then usually sufficient to identify uniquely both the return map and the global torsion. In turn, the return map can be used to estimate the recurrence properties of longer periodic orbits[22] and as an aid to their reconstruction from the time-series data. The relative rotation rates of these additional reconstructed orbits can be computed and compared with those determined from the return map as an added confirmation that the topological properties of the strange attractor have been correctly identified.

To illustrate this procedure we have carried out the computations described above for the Duffing oscillator

$$\begin{aligned}\dot{x}_1&=x_2,\\ \dot{x}_2&=-dx_2-x_1-x_1^3+f\cos(2\pi x_3+\phi),\\ \dot{x}_3&=\omega/2\pi,\end{aligned} \quad (2)$$

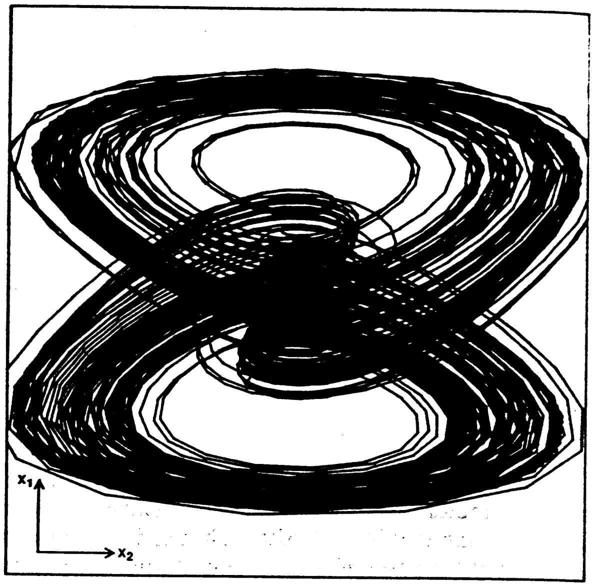

FIG. 1. Projection of a segment of the strange attractor for the Duffing Eqs. (2) onto the x_1-x_2 phase space. The control parameter values are $d=0.2$, $f=27.0$, $\omega=1.330$, and $\phi=0.0$.

with control parameter values $d=0.2$, $f=27.0$, $\omega=1.330$, and $\phi=0.0$. These parameter values lie in the bifurcation tongue with global torsion $T=3$.[19,23] They are far enough along the axis of the tongue that a strange attractor exists. We do not know whether the attractor is hyperbolic and the embedded unstable periodic orbits dense for these parameter values. However, this is not important for reasons explained above.

The Duffing Eqs. (2) were integrated for 2^{13} periods with 2^{13} steps per period. Data were sampled and stored every 2^7 steps, so that 2^6 points were sampled per period. A short segment of the chaotic orbit from the strange attractor, projected onto the x_1-x_2 phase space, is shown in Fig. 1.

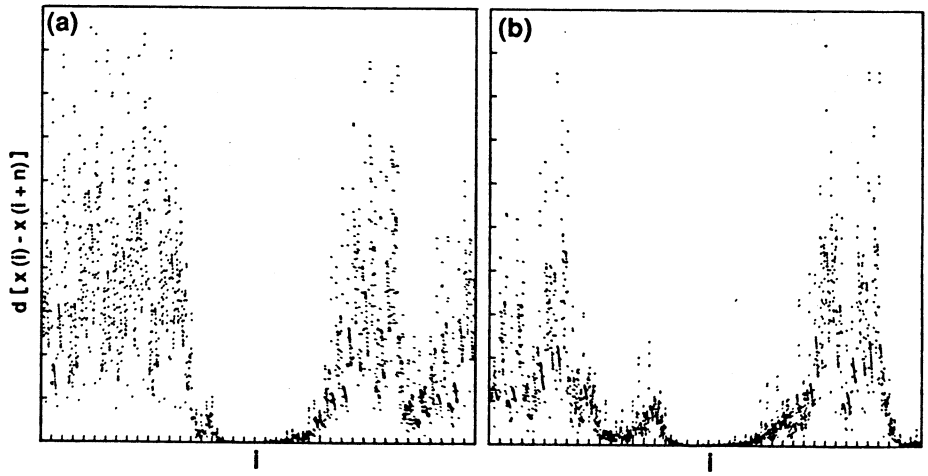

FIG. 2. Distances $d[\mathbf{x}(i)-\mathbf{x}(i+n)]$ plotted as a function of i for fixed $n=kn_0$, with $n_0=2^6$. The windows in these plots show near periodicity over at least a full period in the corresponding segment of the time-series data. The bottom of each window is a good approximation to the nearby unstable periodic orbit. (a) $k=2$ and (b) $k=3$.

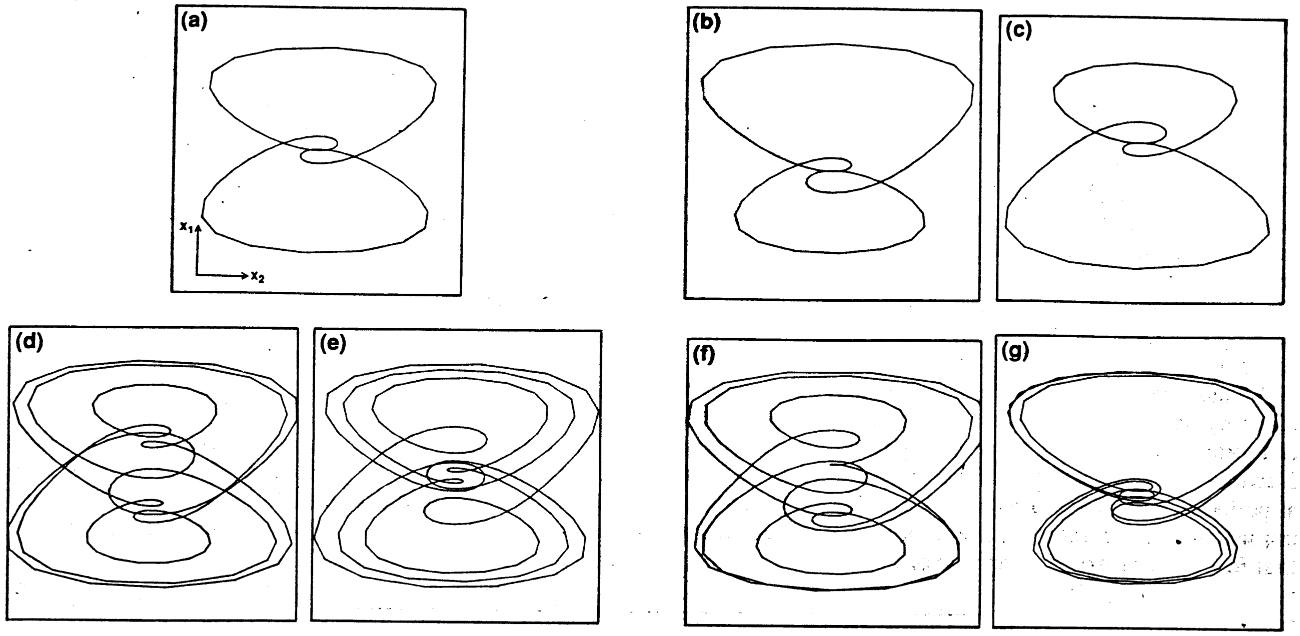

FIG. 3. Some of the periodic orbits extracted from the chaotic time-series data of Fig. 1. (a) Symmetric period-one orbit; (b), (c) asymmetric pair of period-one orbits; (d), (e) symmetric period-three orbits; (f), (g) asymmetric period-three orbits.

Periodic orbits were reconstructed from the sampled data using a standard Euclidean metric. The distances $d[\mathbf{x}(i)-\mathbf{x}(i+n)]$ were plotted as a function of i for fixed $n=kn_0$, with $n_0=2^6$. Samples of such plots are shown in Fig. 2 for $k=2$ and 3. The windows in these plots are clear signatures of near periodicity over several complete periods in the corresponding segment of the time-series data. The segment of length n with the smallest cumulative distance (the bottom of the window) was chosen to represent the nearby unstable periodic orbit. This choice was adequate for reconstructing the orbits. Some of the unstable periodic orbits which were reconstructed by this procedure are shown in Fig. 3. Since the low period orbits are well separated in phase space, the relative rotation rates are insensitive to perturbations such as small noise levels, the approximate reconstruction adopted here, or

TABLE I. Relative rotation rates for all pairs of reconstructed periodic orbits. The global torsion 3 has been subtracted from all relative rotation rates. The orbit (p,n) is the nth orbit of period p extracted from the data. A logical name is assigned to each orbit using the notational conventions proposed earlier. Symmetric orbits are indicated by index γ; asymmetric pairs of orbits are indicated by the indices α, β.

	1.1 $y\gamma$	1.2 $xy\alpha$	1.3 $xy\beta$	2.1 $xy^3\alpha$	2.2 $xy^3\beta$	3.1 $xxy\gamma$	3.2 x^2y^2xy	3.3 x^2y^4	3.4 xy^5	3.5 xy^3xy	3.6 $xy^2\gamma$	4.1	4.2	4.3	5.1	5.2
1.1		1	1	1	1	$\frac{2}{3}$	$\frac{2}{3}$	$\frac{2}{3}$	1	1	$\frac{2}{3}$	1	1	$\frac{3}{4}$	1	1
1.2			1	$\frac{1}{2}$	1	$\frac{2}{3}$	$\frac{2}{3}$	$\frac{2}{3}$	$\frac{2}{3}$	1	$\frac{2}{3}$	$\frac{3}{4}$	1	$\frac{3}{4}$	1	$\frac{3}{5}$
1.3				1	$\frac{1}{2}$	$\frac{2}{3}$	$\frac{2}{3}$	$\frac{2}{3}$	1	$\frac{2}{3}$	$\frac{2}{3}$	1	$\frac{3}{4}$	$\frac{3}{4}$	$\frac{3}{5}$	1
2.1					1	$\frac{2}{3}$	$\frac{2}{3}$	$\frac{2}{3}$	$\frac{2}{3}$	1	$\frac{2}{3}$	$\frac{3}{4}$	1	$\frac{3}{4}$	1	$\frac{3}{5}$
2.2						$\frac{2}{3}$	$\frac{2}{3}$	$\frac{2}{3}$	1	$\frac{2}{3}$	$\frac{2}{3}$	1	$\frac{3}{4}$	$\frac{3}{4}$	$\frac{3}{5}$	1
3.1							$(\frac{2}{3})^2\frac{1}{3}$	$(\frac{2}{3})^2\frac{1}{3}$	$\frac{2}{3}$	$\frac{2}{3}$	$\frac{2}{3}$	$\frac{2}{3}$	$\frac{2}{3}$	$\frac{2}{3}$	$\frac{2}{3}$	$\frac{2}{3}$
3.2								$(\frac{2}{3})^2\frac{1}{3}$	$\frac{2}{3}$	$\frac{2}{3}$	$\frac{2}{3}$	$\frac{2}{3}$	$\frac{2}{3}$	$\frac{2}{3}$	$\frac{2}{3}$	$\frac{2}{3}$
3.3									$\frac{2}{3}$	$\frac{2}{3}$	$\frac{2}{3}$	$\frac{2}{3}$	$\frac{2}{3}$	$\frac{2}{3}$	$\frac{2}{3}$	$\frac{2}{3}$
3.4										1	$\frac{2}{3}$	$\frac{3}{4}$	1	$\frac{3}{4}$	$\frac{2}{3}$	1
3.5											$\frac{2}{3}$	1	$\frac{3}{4}$	$\frac{3}{4}$	1	$\frac{2}{3}$
3.6												$\frac{2}{3}$	$\frac{2}{3}$	$\frac{2}{3}$	$\frac{2}{3}$	$\frac{2}{3}$
4.1													1	$\frac{3}{4}$	1	$\frac{3}{4}$
4.2														$\frac{3}{4}$	$\frac{3}{4}$	1
4.3															1	$\frac{3}{4}$
5.1																1
5.2																

the crude shape of each periodic orbit based on only 2^6 sampled points per period.

The relative rotation rates for all pairs of reconstructed periodic orbits were computed. These indices are presented in Table I. This table also indicates the period of each reconstructed orbit and provides a logical name for all orbits up to period 3 in accordance with the conventions adopted previously.[19] Comparison of this table with a canonical table for the iterated horseshoe return map reveals that the local return map is the iterated horseshoe. This was previously identified as the return map for the Duffing oscillator.[19] This identification requires the global torsion to be 3.

An independent confirmation of this identification was made by using the reconstructed periodic orbits as initial conditions to locate the unstable periodic orbits by a Newton-Raphson procedure. The reconstructed and actual periodic orbits differed by less than 1%. The intertwining matrix for the actual periodic orbits was identical to that for the reconstructed periodic orbits.

In summary, we have shown that it is possible to construct topological invariants for a strange attractor far from the onset of chaos. These invariants are functions of the embedded unstable periodic orbits, which are dense if the strange attractor is hyperbolic. The topological invariants are the relative rotation rates for pairs of periodic orbits reconstructed from time series data. The *topological invariants for a relatively small number of periodic orbits are sufficient* to identify the return mapping mechanism responsible for creation of the strange set as well as the global torsion of the flow. The feasibility demonstration was carried out for the Duffing oscillator which is a good model for chaotic single-mode string dynamics.[24,25]

We would like to thank D. Auerbach, E. J. Kostelich, D. P. Lathrop, and G. R. Hall for useful discussions. We also thank N. B. Abraham and A. M. Albano. This work was supported in part by National Science Foundation Grant No. PHY 88-43235.

[1] M. J. Feigenbaum, J. Stat. Phys. **19**, 25 (1978).
[2] S. J. Shenker, Physica **5D**, 405 (1982); **5D**, 411 (1982).
[3] P. Bak and J. Bruinsma, Phys. Rev. Lett. **49**, 249 (1982).
[4] P. Bak, T. Bohr, and M. H. Jensen, Phys. Scr. **T9**, 50 (1985).
[5] P. Cvitanovic, G. H. Gunaratne, and I. Procaccia, Phys. Rev. A **38**, 1503 (1988).
[6] G. H. Gunaratne, M. H. Jensen, and I. Procaccia, Nonlinearity **1**, 157 (1988).
[7] G. H. Gunaratne, P. S. Linsay, and M. J. Vinson, Phys. Rev. Lett. **63**, 1 (1989).
[8] C. Grebogi, E. Ott, and J. A. Yorke, Phys. Rev. A **37**, 1711 (1988).
[9] P. Cvitanovic, Phys. Rev. Lett. **61**, 2729 (1989).
[10] D. Auerbach, P. Cvitanovic, J.-P. Eckmann, G. H. Gunaratne, and I. Procaccia, Phys. Rev. Lett. **58**, 2387 (1987).
[11] I. Procaccia, Nucl. Phys. **B2**, 527 (1987).
[12] C. Grebogi, E. Ott, and J. A. Yorke, Phys. Rev. A **36**, 3522 (1988).
[13] G. H. Gunaratne and I. Procaccia, Phys. Rev. Lett. **59**, 1377 (1987).
[14] R. Devaney and Z. Nitecki, Commun. Math. Phys. **67**, 137 (1979).
[15] Z. Nitecki, *Differentiable Dynamics* (MIT, Cambridge, MA 1971).
[16] J. S. Birman and R. F. Williams, Topology **22**, 47 (1983).
[17] P. J. Holmes and R. F. Williams, Arch. Ration. Mech. Anal. **90**, 115 (1985).
[18] H. G. Solari and R. Gilmore, Phys. Rev. A **37**, 3096 (1988).
[19] H. G. Solari and R. Gilmore, Phys. Rev. A **38**, 1566 (1988).
[20] D. P. Lathrop and E. J. Kostelich, Phys. Rev. A **40**, 4028 (1989).
[21] S. Smale, Bull. Am. Math. Soc. **73**, 747 (1967).
[22] L. A. Smith, in *Proceedings of the Bryn Mawr Conference on Quantitative Measures of Dynamical Complexity in Nonlinear Systems*, edited by N. B. Abraham, A. M. Albano, A. Passamente, and P. E. Rapp (Plenum, New York, in press).
[23] U. Parlitz and W. Lauterborn, Phys. Lett. **107A**, 351 (1985).
[24] N. B. Tufillaro, Am. J. Phys. **57**, 408 (1989).
[25] T. C. Molteno and N. B. Tufillaro, J. Sound Vibration **137** (2), 327 (1990).